Co-Doped (La, Sr)$TiO_{3-\delta}$: A High Curie Temperature Diluted Magnetic System with Large Spin Polarization

G. Herranz,[1,*] R. Ranchal,[2] M. Bibes,[3] H. Jaffrès,[1] E. Jacquet,[1] J.-L. Maurice,[1] K. Bouzehouane,[1] F. Wyczisk,[4] E. Tafra,[5] M. Basletic,[5] A. Hamzic,[5] C. Colliex,[6] J.-P. Contour,[1] A. Barthélémy,[1] and A. Fert[1]

[1]*Unité Mixte de Physique CNRS/Thales, Route départementale 128, 91767 Palaiseau Cedex, France*
[2]*Departamento de Física de Materiales, Facultad de Ciencias Físicas (UCM), Avenida Complutense, s/n 28040-Madrid, Spain*
[3]*Institut d'Electronique Fondamentale, Université Paris-Sud, 91405 Orsay, France*
[4]*Thales Research and Technology France, Route départementale 128, 91767 Palaiseau Cedex, France*
[5]*Department of Physics, Faculty of Sciences, University of Zagreb, Bijenicka 32—P.O.B. 331 HR-10002 Zagreb, Croatia*
[6]*Laboratoire de Physiques des Solides, Université Paris-Sud-UMR 8502, 91405 Orsay, France*

(Received 11 August 2005; published 19 January 2006)

We report on tunneling magnetoresistance (TMR) experiments that demonstrate the existence of a significant spin polarization in Co-doped (La, Sr)$TiO_{3-\delta}$ (Co-LSTO), a ferromagnetic diluted magnetic oxide system (DMOS) with high Curie temperature. These TMR experiments have been performed on magnetic tunnel junctions associating Co-LSTO and Co electrodes. Extensive structural analysis of Co-LSTO combining high-resolution transmission electron microscopy and Auger electron spectroscopy excluded the presence of Co clusters in the Co-LSTO layer and thus, the measured ferromagnetism and high spin polarization are intrinsic properties of this DMOS. Our results argue for the DMOS approach with complex oxide materials in spintronics.

DOI: 10.1103/PhysRevLett.96.027207 PACS numbers: 75.50.Pp, 75.47.Pq, 85.75.Mm

The research of ferromagnetic semiconductors is an important challenge in spintronics nowadays. Since ferromagnetic properties have been found in Mn-GaAs [1], several types of other diluted magnetic semiconductors have been investigated. The discovery of room temperature ferromagnetism in Co-doped anatase TiO_2 [2] has triggered an intense research on other diluted magnetic oxide systems (DMOS). Some recent experiments have also suggested the existence of ferromagnetism in $La_{0.5}Sr_{0.5}TiO_{3-\delta}$ doped with Co [3,4], i.e., a DMOS in which the host oxide is not a semiconductor but a strongly correlated metal [5]. Several models of ferromagnetism have been proposed for these DMOS, including models based on a new type of exchange interactions via shallow donors (associated with oxygen vacancies) [6].

Application of DMOS to spintronics requires not only ferromagnetism but also spin polarization of the carriers. This spin polarization can be studied by several techniques. For instance, x-ray magnetic circular dichroism is one of the best tools to detect the coupling between delocalized *sp* carriers and localized *d* electrons and was successfully applied in transition metal doped ZnO [7]. On the other hand, it has been argued that anomalous Hall effect (AHE) should be observed in these compounds. Nevertheless, the concomitant observation in Co-doped TiO_2 of parasitic superparamagnetic metallic Co clusters and AHE has cast doubts on the usefulness of AHE to unambiguously demonstrate intrinsic spin-polarization in DMOS [8]. A more direct way is provided by tunneling magnetoresistance (TMR) measurements that can probe directly the spin polarization involved in spintronics experiments. This is the way we have taken to investigate the ferromagnetism and the spin polarization in the (La, Sr)$Ti_{1-x}Co_xO_{3-\delta}$ (Co-LSTO, $x \simeq 0.01$) DMOS.

In this Letter we thus report on the growth of Co-LSTO films, their magnetic and structural characterizations, on the fabrication of tunnel junctions composed of Co-LSTO and Co electrodes separated by a $LaAlO_3$ (LAO) barrier, and on the TMR experiments performed on these junctions and their interpretation.

We have deposited Co-LSTO epitaxial thin films on $SrTiO_3(001)$ substrates from a target with composition $La_{0.37}Sr_{0.63}Ti_{0.98}Co_{0.02}O_3$ by pulsed laser deposition (PLD) [9] (i.e., $x \simeq 0.02$). The heterostructures elaborated for the definition of magnetic tunnel junctions (MTJs) were fabricated by first growing Co-LSTO(150 nm)/LAO(1.6 nm) bilayers at $P_{O_2} = 6 \times 10^{-7}$ mbar by PLD and subsequently sputter depositing *ex situ* a Co(12 nm)/CoO(3 nm)/Au(15 nm) stack. The CoO was intended to magnetically pin the top Co electrode by exchange bias. The heterostructures were then patterned into MTJs with size ranging from 6 to 128 μm^2 by an advanced photolithography process [10].

We have investigated the structural properties and the homogeneity of the chemical composition of various Co-LSTO films by combining several advanced characterization tools. Auger electron spectroscopy (AES) mappings were performed over regions of size up to 10×10 μm^2 to detect La, Sr, Ti, O, and Co elements. The resulting elemental mappings were homogeneous and did not show any contrast (see, for instance, a mapping for Co in the inset of Fig. 1). The AES signals were also measured in real time while sputtering the films with Ar ions accelerated at 2 keV; see Fig. 1. The AES signals remain roughly con-

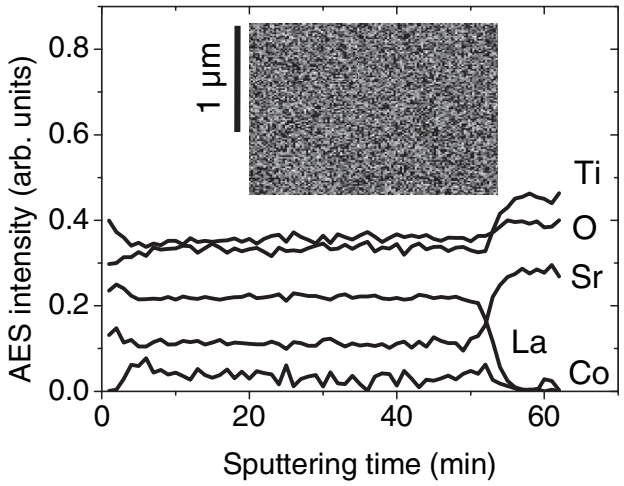

FIG. 1. Auger intensity for several elements, measured as a function of the sample etching time, for a Co-LSTO film of thickness $t = 130$ nm grown at $P_{O_2} = 6 \times 10^{-7}$ mbar. Inset: AES mapping of Co in the same film.

stant, indicating a homogeneous distribution of the different elements, until a sputtering time of about 50 min when the La and Co levels decay steadily to zero, while the Sr and Ti levels increase and then stay constant. This signals the interface between the Co-LSTO film and the STO substrate. The level of the Co was estimated to be around $x = 0.01$, which is somehow lower than the nominal $x = 0.02$.

We have also investigated the microstructure of Co-LSTO thin films using transmission electron microscopy (TEM) and high-resolution TEM (HRTEM) experiments combined with electron energy loss spectroscopy (EELS) measurements. No parasitic phase [e.g., Co clusters, (La, Sr)CoO_3, etc.] was detected by TEM or HRTEM. In Fig. 2(a) we show a HRTEM image of the Co-LSTO/STO interface in the [100] zone evidencing a good epitaxial quality. The absence of Co-rich regions was further confirmed by low-magnification EELS elemental mappings in cross section [see in Figs. 2(b)–2(d)]. The signal in the Co image is pure noise in the used recording conditions (0.5 s pixel^{-1}).

Finally we have also analyzed the fine structure of the Ti edge in the EELS spectra, which is characteristic of its valence. We estimate the 3+/4+ ratio in our samples by considering the Ti edges we have recorded [Fig. 2(e)], as a linear combination of the edges of pure Ti^{3+} and Ti^{4+} recorded on standards with approximately the same energy resolution (0.8 eV). We find a 3+/4+ ratio of ~3:1, corresponding to an average valence of ~3.25+ for the Ti ions. If we assume the La/Sr ratio to be ~0.58 as in the target, the Ti valence should be ~3.63+. This difference can be explained by the presence of oxygen vacancies promoted by the low growth pressure, creating electrons that populate the Ti 3*d* band. The oxygen deficiency necessary to account for a valence of 3.25+ is $\delta \simeq 0.19$ that is

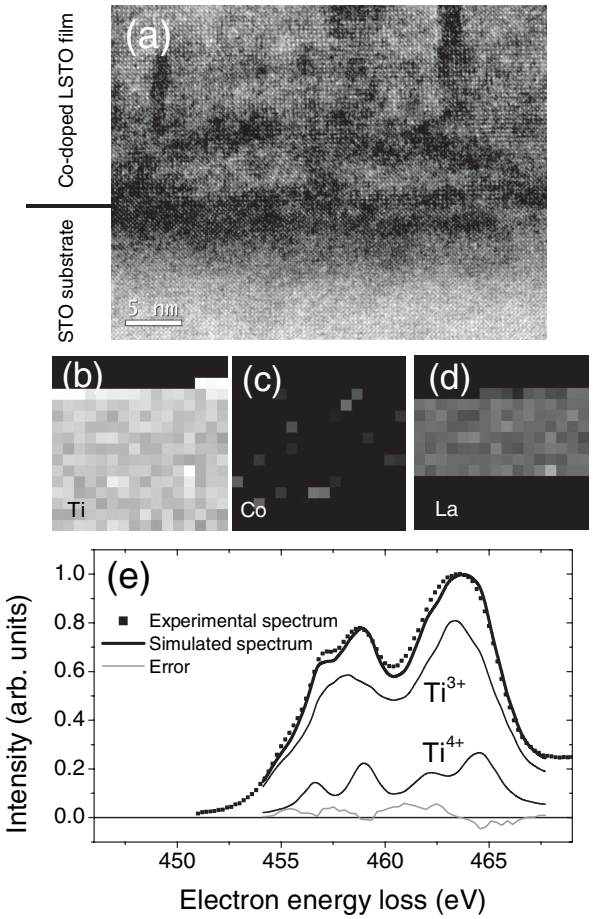

FIG. 2. (a) HRTEM image of a LSTO/STO system ($t =$ 100 nm, $P_{O_2} = 6 \times 10^{-7}$ mbar) in cross section in [100] zone. (b)–(d) EELS element-selective images. Grey levels are proportional to the [element]/[oxygen] ratio. Black is zero; white is 50% in Ti and La images, 1% in Co image. The pixel size is 12 nm. (e) Experimental and simulated EELS spectra at the Ti-$L_{2,3}$ edge, together with reference spectra for Ti^{3+} and Ti^{4+} [adapted from Ref. [17]].

close to the value found by Muller *et al.* in $SrTiO_{3-\delta}$ films grown in similar conditions [11].

To summarize this structural part, we can conclude from the HRTEM pictures and the elemental mappings obtained by AES and EELS that the films are of very good structural quality, with no extended defects and, more importantly, that the Co distribution is homogeneous in the film. No Co-rich regions larger than ~10 nm are present.

In Fig. 3(a), we show a typical ferromagnetic hysteresis cycle measured at room temperature for a 130 nm Co-LSTO film grown at $P_{O_2} = 6 \times 10^{-7}$ mbar. The saturation magnetization (M_S) for this film is about 4.5 emu cm^{-3} (see inset) and was found to increase when P_{O_2} decreased from $P_{O_2} = 5 \times 10^{-4}$ to 6×10^{-7} mbar. This suggests some role of oxygen vacancies on magnetism. From the Co concentration measured by AES, we can calculate that the magnetization of the low-P_{O_2} films corresponds to 3–4 μ_B/Co, which is fairly larger than the moment of

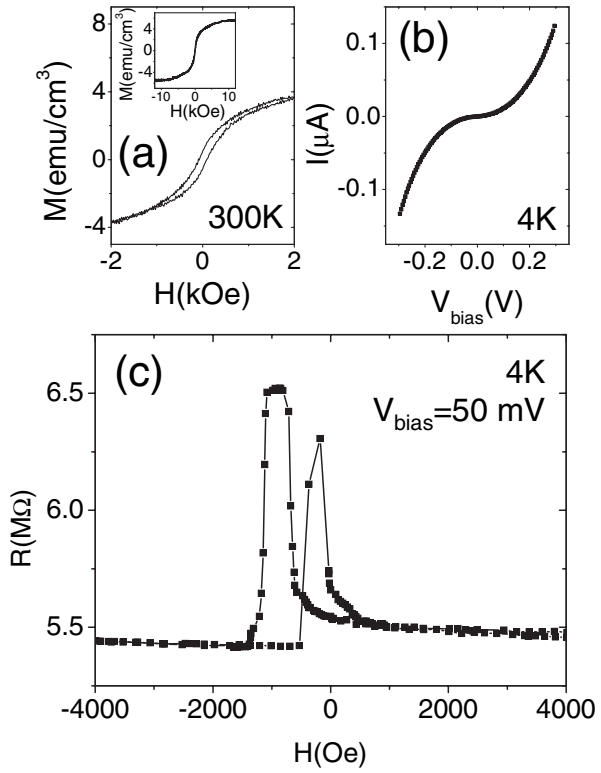

FIG. 3. (a) Magnetization hysteresis cycle measured with an alternating gradient force magnetometer (AGFM) for a 130 nm Co-LSTO film grown at $P_{O_2} = 6 \times 10^{-7}$ mbar, with the magnetic field applied in plane. Inset: same $M(H)$ up to saturation. (b) I-V curve of a Co-LSTO/LAO/Co tunnel junction measured at 4 K and in a field $H = 6000$ Oe. (c) Field dependence of the resistance of a Co-LSTO/LAO/Co magnetic tunnel junction (size 64 μm^2), at 4 K and bias voltage of 50 mV.

metallic Co (1.7 μ_B). This may be an indication of magnetic interactions between Co ions mediated by carriers at the 3*d*-Ti conduction band. This picture is supported by some preliminary nuclear magnetic resonance (NMR) measurements on our Co-LSTO films showing the presence of ferromagnetic Ti, as indicated by observation of ^{47}Ti and ^{49}Ti NMR signals corresponding to a hyperfine field of 12 T at 4.2 K [12].

Figure 3(c) shows a TMR curve recorded at 4 K in one of our Co-LSTO/LAO/Co/CoO/Au MTJs (size: 64 μm^2). The curve was obtained at $V_{\text{bias}} = 50$ mV after field cooling in 6 kOe. The $R(H)$ curves are shifted respect to the $H = 0$ axis, which is due to the exchange bias induced by the CoO layer on the Co electrode and, for the Co-LSTO electrode, to the dipolar field generated by the Co layer in the mesa structure of the junction. Note that a plateau is clearly observed in the antiparallel state, which suggests that the magnetization of the Co-LSTO layer is almost saturated in this field range under the action of the applied field and the dipolar field induced by the Co layer. The I(V) curves [see Fig. 3(b)] are nonlinear, indicative of tunnel transport. Our first conclusion is that large TMR effects (up to ~19%) are observed and demonstrate the spin polarization of the carriers in the Co-LSTO electrode. The existence of such spin polarization as well as a robust magnetism for a Co concentration of ~1 at.% allows excluding short-range interactions such as conventional superexchange or double-exchange to be at the origin of ferromagnetism in this compound. We discuss below the quantitative determination of the spin polarization.

A striking result of our tunneling experiments is the bias dependence of the TMR; see Fig. 4(a). This type of bias dependence is usually observed when there is a significant contribution of impurity-assisted (or defect-assisted) tunneling. A clear interpretation of this bias dependence has been given by Tsymbal *et al.* for Ni/NiO/Co nanojunctions in which the small size (0.01 μm^2) of the junctions allowed these authors to assume resonant tunneling via a single localized level (a single level in a given junction) [13]. Here we use the extension of the model worked out by Garcia *et al.* [14] to describe the situation with still single-impurity-assisted tunneling but localized levels distributed in a band. In our junctions, the localized levels could be due to O vacancies promoted by the low oxygen pressure growth conditions. We assume a distribution of localized levels within a band of width W, centered at a mean energy ε_C from the Fermi energy level E_F of the electrodes and having a Lorentzian energy distribution. The conductance per impurity can be expressed as

$$G(\sigma, \sigma') = \frac{4e^2}{h} \frac{\Gamma_{L\sigma}\Gamma_{R\sigma'}}{\Gamma_{L\sigma} + \Gamma_{R\sigma'}} \times \frac{\Gamma_{L\sigma} + \Gamma_{R\sigma'} + W}{4(\varepsilon - \varepsilon_C)^2 + (\Gamma_{L\sigma} + \Gamma_{R\sigma'} + W)^2}, \quad (1)$$

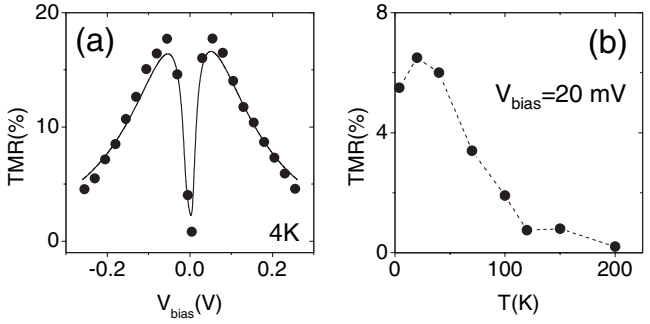

FIG. 4. (a) TMR bias dependence of a 64 μm^2 Co-LSTO/LAO/Co MTJ. The solid line corresponds to the fit obtained taking into account a Lorentzian damping function with a characteristic value $V_{1/2} = 150$ mV and the following parameter values: $P_L = -0.3$, $P_R = -0.78$, $\Gamma_L = (\Gamma_{L\uparrow} + \Gamma_{L\downarrow})/2 = 0.88$ meV, $\Gamma_R = (\Gamma_{R\uparrow} + \Gamma_{R\downarrow})/2 = 5.7$ meV, $\varepsilon_C = 1.65$ meV. Optimal fittings were obtained by assuming a narrow energy band ($W = 0$), corresponding to the case of impurities occupying the same energy level (i.e., the mean spatial separation of impurities might be too large to induce any overlapping and hybridization between two neighboring defects). (b) Temperature dependence of a Co-LSTO/LAO/Co junction (size: 12 μm^2) at bias $V = 20$ mV.

where $\Gamma_{L\sigma}/\hbar$, $\Gamma_{R\sigma'}/\hbar$ are the leak rates of an electron from the localized state into the left (L) or right (R) electrode, respectively, and σ, σ' refer to the spin state ($\uparrow, \downarrow$) of the left (right) electrode. This resonant tunneling model includes six parameters, namely, $\Gamma_{L\sigma}$, $\Gamma_{R\sigma'}$, W, ε_C. The spin polarizations of the leak rates, $P_L = (\Gamma_{L\uparrow} - \Gamma_{L\downarrow})/(\Gamma_{L\uparrow} + \Gamma_{L\downarrow})$ and $P_R = (\Gamma_{R\uparrow} - \Gamma_{R\downarrow})/(\Gamma_{R\uparrow} + \Gamma_{R\downarrow})$ are the spin polarizations of the left and right electrodes. All the TMR bias dependences can be fitted with Eq. (1) and with a convenient set of parameters, which indicates that the main contribution to the tunneling comes from this process. We show a typical example in Fig. 4(a). The most remarkable result is that we extract almost the same spin polarization for each electrode from fits of the bias dependence of TMR in several junctions, i.e., $P_L = -0.25 \pm 0.05$ and $P_R = -0.8 \pm 0.02$ (or $P_L = +0.25 \pm 0.05$ and $P_R = +0.8 \pm 0.02$, since we cannot determine the sign of each polarization). However, TMR measurements obtained on $La_{2/3}Sr_{1/3}MnO_3$/LAO/Co MTJs indicate a negative spin polarization of about $P \simeq -12\%$ at the Co/LAO interface [15]. We can thus suppose that both P_L and P_R are negative and that the smallest spin polarization (in absolute value) corresponds to that of the Co/LAO interface, that is, $P_{\mathrm{Co/LAO}} = -0.25 \pm 0.05$. This would therefore imply a spin polarization of -0.8 ± 0.02 for the Co-LSTO/LAO interface. This observation of a spin polarization undoubtedly argues for an intrinsic origin of ferromagnetism in Co-LSTO.

The last question is the origin of these impurity states. We recall that in order to optimize the magnetic properties of the Co-LSTO films the Co-LSTO/LAO bilayers were grown at extremely low oxygen pressures (6×10^{-7} mbar). Thus, the barriers were not grown in standard conditions, and very likely contain oxygen vacancies that create defect states within the LAO gap. In Fig. 4(b) we present the temperature dependence of the TMR of a 12 μm^2 junction at $V_{\mathrm{bias}} = 20$ mV. The TMR decreases rapidly with T and becomes vanishingly small above 200 K. This behavior is unexpected since Co-LSTO is ferromagnetic at 300 K [see Fig. 3(a)] and the Curie temperature of Co is far above room temperature. There are several possible origins for this behavior. First, we note that the pinning by exchange bias of the Co-top electrode in our structures disappears at $T > 150$ K, which can lead to very similar values of the coercive fields of Co and Co-LSTO above this temperature and, consequently, to the absence of a field range with antiparallel orientation. Another origin may be related to the onset of thermally assisted spin flips on impurity levels inside the barrier, which may be detrimental to the spin polarization of the tunneling current as observed in MnAs/GaAs(AlAs)/MnAs MTJs [14]. In a model of resonant tunneling through localized states as well as in the case of sequential processes through an energy band, TMR subsists unless the tunneling time $\tau_n = \hbar/(\Gamma_L + \Gamma_R)$ of the particle exceeds its spin lifetime τ_{sf}. The rapid decrease of TMR with temperature might indicate the effects of some thermally assisted spin flip mechanisms drastically shortening the spin lifetime with temperature. Finally one must not discard the possibility of a degradation of the spin polarization at the Co-LSTO/LAO interfaces, as observed in other ferromagnetic oxides [16]. More experiments are foreseen in order to clarify the role of the Co-top electrode pinning or the impurity levels in the barrier in both the bias and temperature dependence of the MR of Co-LSTO-based MTJs.

In summary, we have reported on TMR results indicating a significant spin polarization of the diluted magnetic oxide system Co-LSTO. By HRTEM, EELS, AES, and AGFM measurements, we exclude Co segregation as the origin of the ferromagnetism and TMR in Co-LSTO, and we conclude that the spin polarization as well as the ferromagnetism are intrinsic properties of this DMOS. Our results bring strong arguments for the DMOS approach with complex oxide materials in spintronics.

We are grateful to P. Berthet, C. Pascanut, and N. Dragoe for providing the Co-LSTO target. G. Herranz acknowledges financial support from Ministère de l'Education Nationale, de l'Enseignement Supérieur et de la Recherche (France), and R. Ranchal thanks Universidad Complutense de Madrid and the Spanish Project No. MAT 2001-3554-CO2 for partially supporting her stay at UMR137, CNRS-Thales at Orsay, France.

*Corresponding author.
Electronic address: gervasi.herranz@gmail.com

[1] H. Ohno *et al.*, Appl. Phys. Lett. **69**, 363 (1996).
[2] Y. Mastumoto *et al.*, Science **291**, 854 (2001).
[3] Y. G. Zhao *et al.*, Appl. Phys. Lett. **83**, 2199 (2003).
[4] P. T. Qiao *et al.*, Thin Solid Films **468**, 8 (2004).
[5] Y. Tokura *et al.*, Phys. Rev. Lett. **70**, 2126 (1993).
[6] J. M. D. Coey, M. Venkatesan, and C. B. Fitzgerald, Nat. Mater. **4**, 173 (2005).
[7] K. Ando *et al.*, J. Appl. Phys. **89**, 7284 (2001).
[8] S. R. Shinde *et al.*, Phys. Rev. Lett. **92**, 166601 (2004).
[9] R. Ranchal *et al.*, J. Appl. Phys. **98**, 013514 (2005).
[10] M. Bowen *et al.*, Appl. Phys. Lett. **82**, 233 (2003).
[11] D. A. Muller, N. Nakagawa, A. Ohtomo, J. L. Grazul, and H. Y. Hwang, Nature (London) **430**, 657 (2004).
[12] E. Jedryka and M. Wojcik (private communication).
[13] E. Y. Tsymbal, A. Sokolov, I. F. Sabirianov, and B. Doudin, Phys. Rev. Lett. **90**, 186602 (2003).
[14] V. Garcia *et al.*, Phys. Rev. B **72**, 081303(R) (2005).
[15] V. Garcia *et al.*, Appl. Phys. Lett. **87**, 212501 (2005).
[16] M. Bibes *et al.*, Phys. Rev. Lett. **87**, 067210 (2001).
[17] A. Ohtomo, D. A. Muller, J. L. Grazul, and H. T. Hwang, Nature (London) **419**, 378 (2002).